EXPERIMENTAL AND FINITE ELEMENT STUDY OF A STANDING TORUS UNDER NORMAL AND TANGENTIAL LOADS

Donald R. Flugrad and Bruce A. Miller
Iowa State University

EXPANDED ABSTRACT

There continues to exist a strong interest in the load deflection attributes of both automotive and aircraft tires. Considerations of safety, handling and performance during such maneuvers as landing, braking and cornering are intimately tied to the adequacy of a vehicle's tire design. In the past, the qualitative and quantitative information needed for a basic understanding of tire characteristics has been derived by strictly empirical methods. Of late, however, numerical techniques such as finite element analysis have been brought to bear on certain aspects of the problem.

This paper describes work that is presently in progress at Iowa State University to determine the effect of a combined external load consisting of a normal component and a tangential braking force applied to an inflated torus. Experimental results obtained by photographic study of the contact area between the torus and load plate are presented as well as measurements of the vertical and horizontal displacement of the torus under load. A numerical procedure for displacement analysis is developed in which the finite element program STAGS (Structural Analysis of General Shells) is used in an iterative manner to produce a flat, horizontal footprint surface under force loading. The redistributed force distribution obtained by the iterative process is displayed along with computed meridional and circumferential stresses. Finally, an extension of the iterative method is introduced which eliminates the need to experimentally determine the footprint area.

LINE DRAWING OF TEST FIXTURE

Figure 1 shows the torus mounted on a rim and axle. The axle is clamped to the frame to prevent rotation of the unit. Two load tables work independently to produce an externally applied load on the torus. The table directly below the torus acts through the pulleys at the top of the fixture to pull the plate in contact with the torus upward, providing a normal load. The table shown to the left of the fixture is then loaded to exert a tangential force in the fore-aft or braking direction.

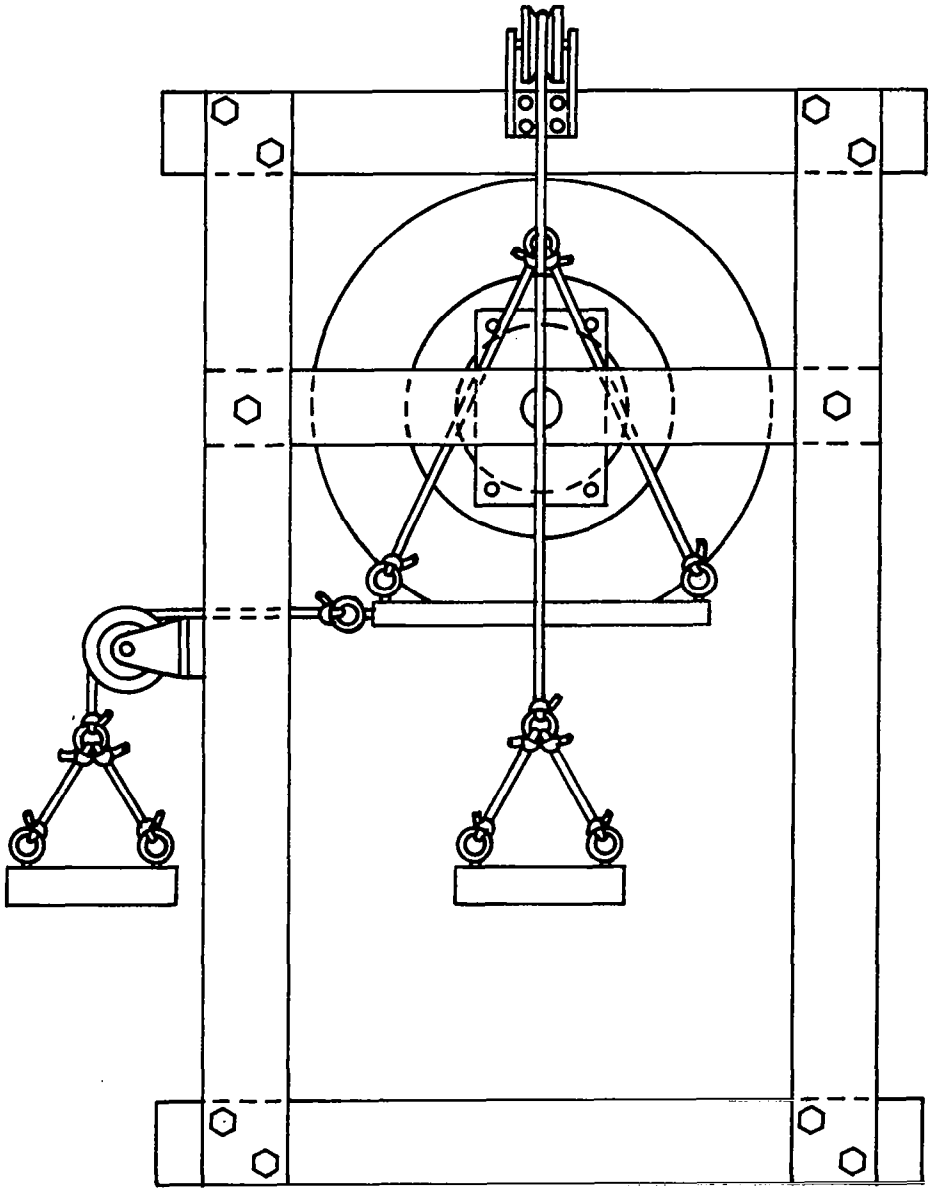

Figure 1

PHOTOGRAPH OF TEST FIXTURE

The actual test fixture is depicted in Figure 2 with weights mounted on the normal load table directly below the 8.00 × 20 inner tube used as the torus. A plastic milk container is shown in place of the tangential load table of Figure 1. By introducing water into the milk container, it is possible to vary the tangential load continuously instead of incrementally as would be the case if weights were placed on a load table. The plate in contact with the torus is made of transparent lucite allowing photographs of the footprint area to be taken from below the plate. Graph paper "targets" are affixed to the lucite plate for the purpose of tracking the vertical and horizontal displacement of the plate under prescribed load conditions. The manometer at the right is used to monitor the internal pressure of the torus.

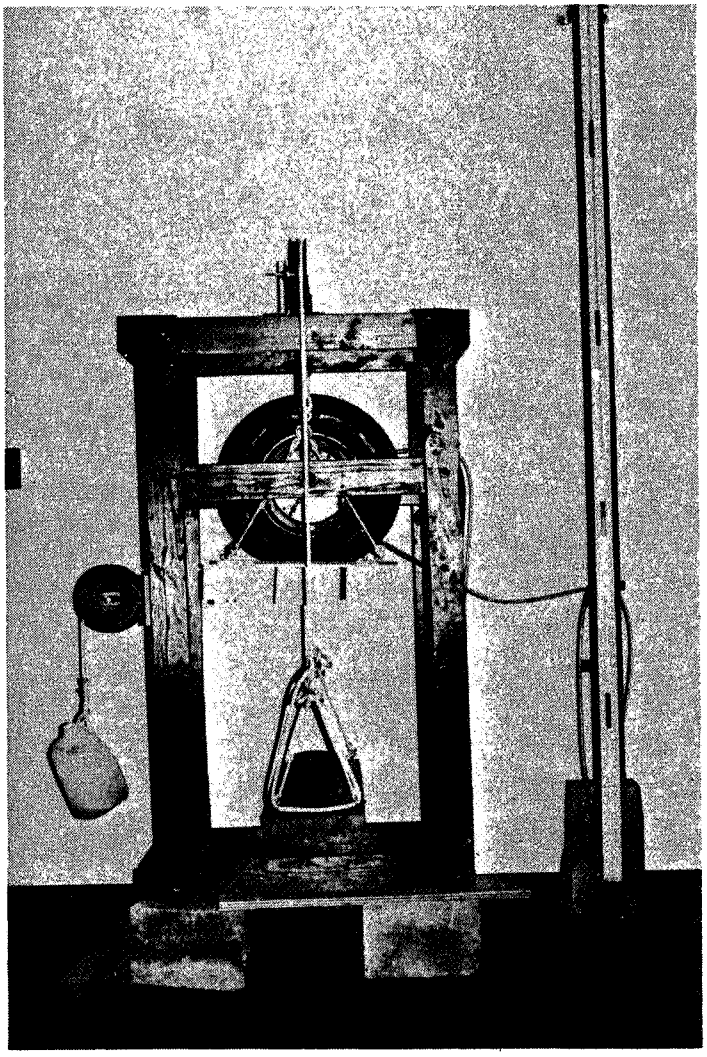

Figure 2

PHOTOGRAPHS OF FOOTPRINT AREAS

The two photographs of Figure 3 show footprint areas viewed through the transparent lucite plate. In both cases the torus is subjected to a normal load of 70 N and an internal pressure of 3450 Pa. Figure 3(a) was taken with no tangential load applied, and figure 3(b) shows the footprint area produced when a tangential load equal to 80% of the normal load is added. The photographs show that the contact area for each case is generally elliptical in shape. Closer inspection of the two photos verifies that there is little if any distortion introduced by the inclusion of a tangential component of force acting on the torus.

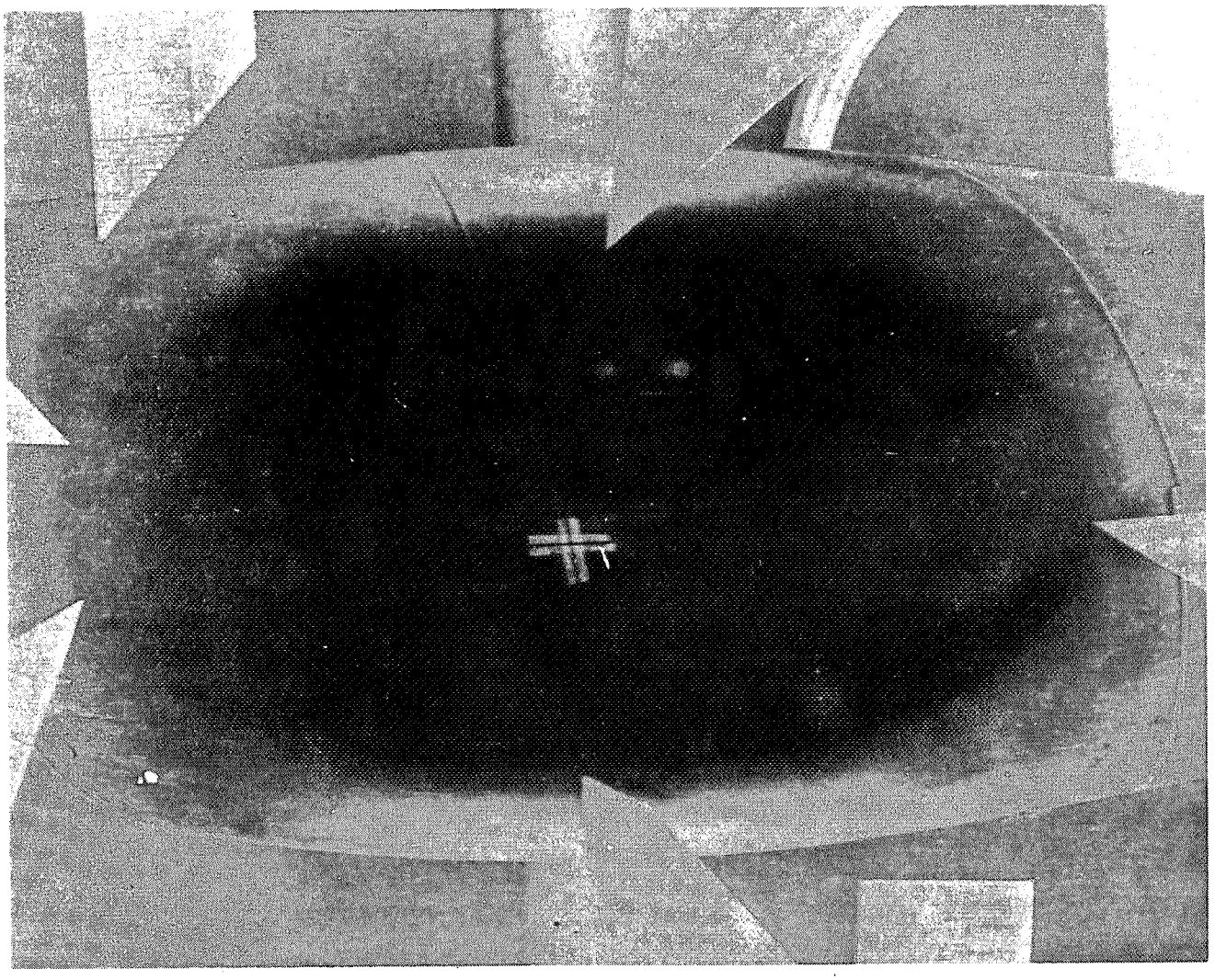

(a) Load = 70 N; braking = 0%; inflation = 3450 Pa.

Figure 3

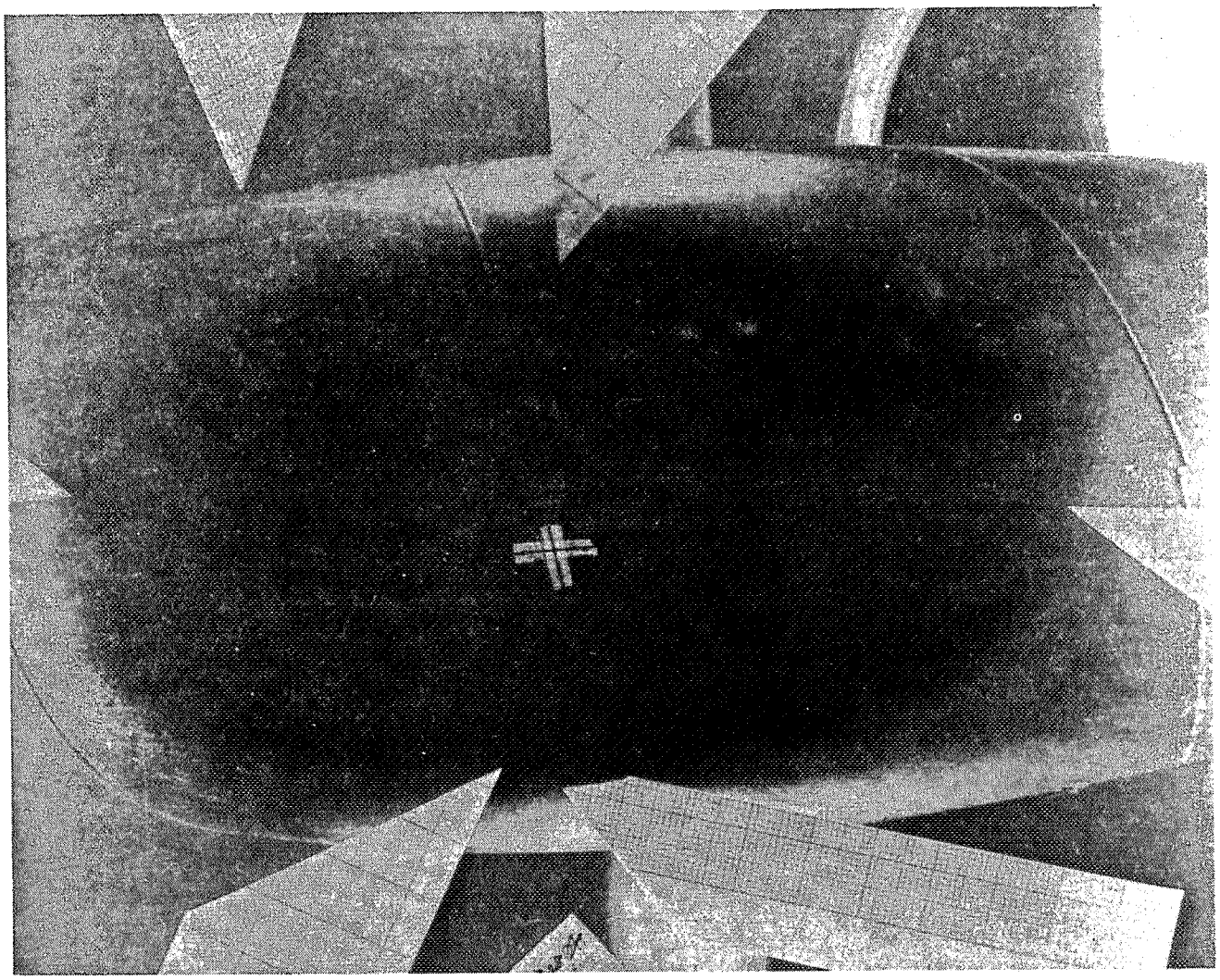

(b) Load = 70 N; braking = 80%; inflation = 3450 Pa.

Figure 3

EXPERIMENTAL MEASUREMENT OF DISPLACEMENT

The experimental set-up for the measurement of vertical and horizontal displacements of the torus under prescribed load conditions is depicted in Figure 4. In actuality the center of the inner tube on its rim and axle is held stationary and the displacement of the lucite plate in contact with the torus is measured. Three graph paper "targets" are attached to the load plate, two of which are visible hanging from the front edge of the plate in the photograph. The third is attached to the back edge of the plate. Three separate optical devices are trained on the grid patterns of the "targets" to record vertical and horizontal displacements of three distinct points on the plate as normal and tangential braking forces are applied to the torus. Only two of the three optical devices appear in the photo. The third, a surveying transit with a much longer focal length, is stationed some distance from the test fixture. The three separate measurements of displacement are then used to estimate the vertical and horizontal movement of a point located at the center of the footprint area.

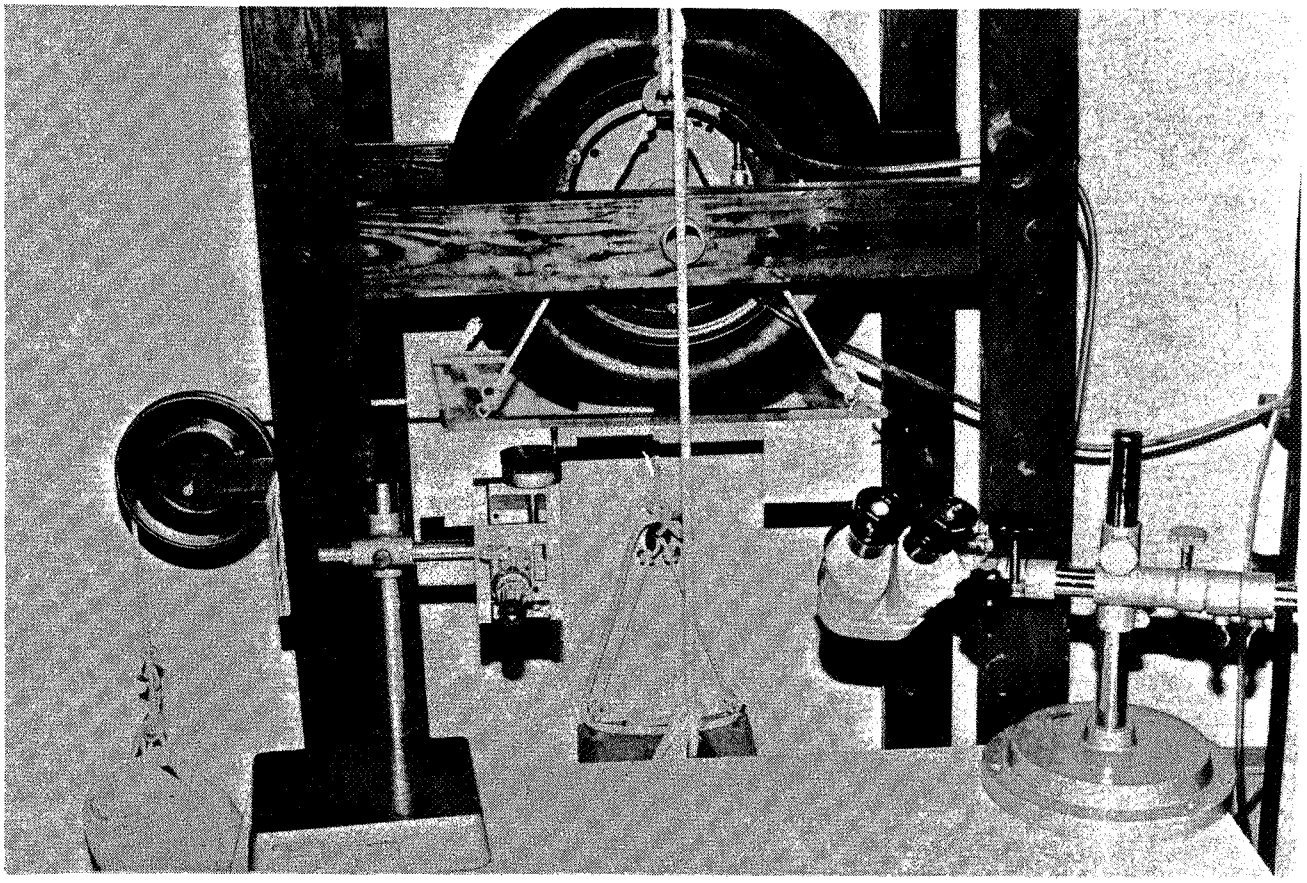

Figure 4

VERTICAL DISPLACEMENT OF TORUS

The graph of Figure 5 illustrates the relationship between the vertical displacement of the torus and the magnitude of the applied tangential braking force for a constant normal load of 70 N. Experimental results plotted on the graph are those obtained by the set-up of Figure 4. The solid line represents a least squares linear fit of the experimental data. Also shown are results obtained from STAGS, a finite element program particularly suited for analysis of plates and shells, for three different tangential load cases. The tangential force associated with the horizontal axis is a non-dimensional quantity which represents the braking force as a decimal fraction of the applied normal load. It is evident that the vertical displacement of the torus is relatively insensitive to the tangential force applied. It is also clear that the finite element analysis predicts a vertical displacement which is consistently less than that obtained by measurement.

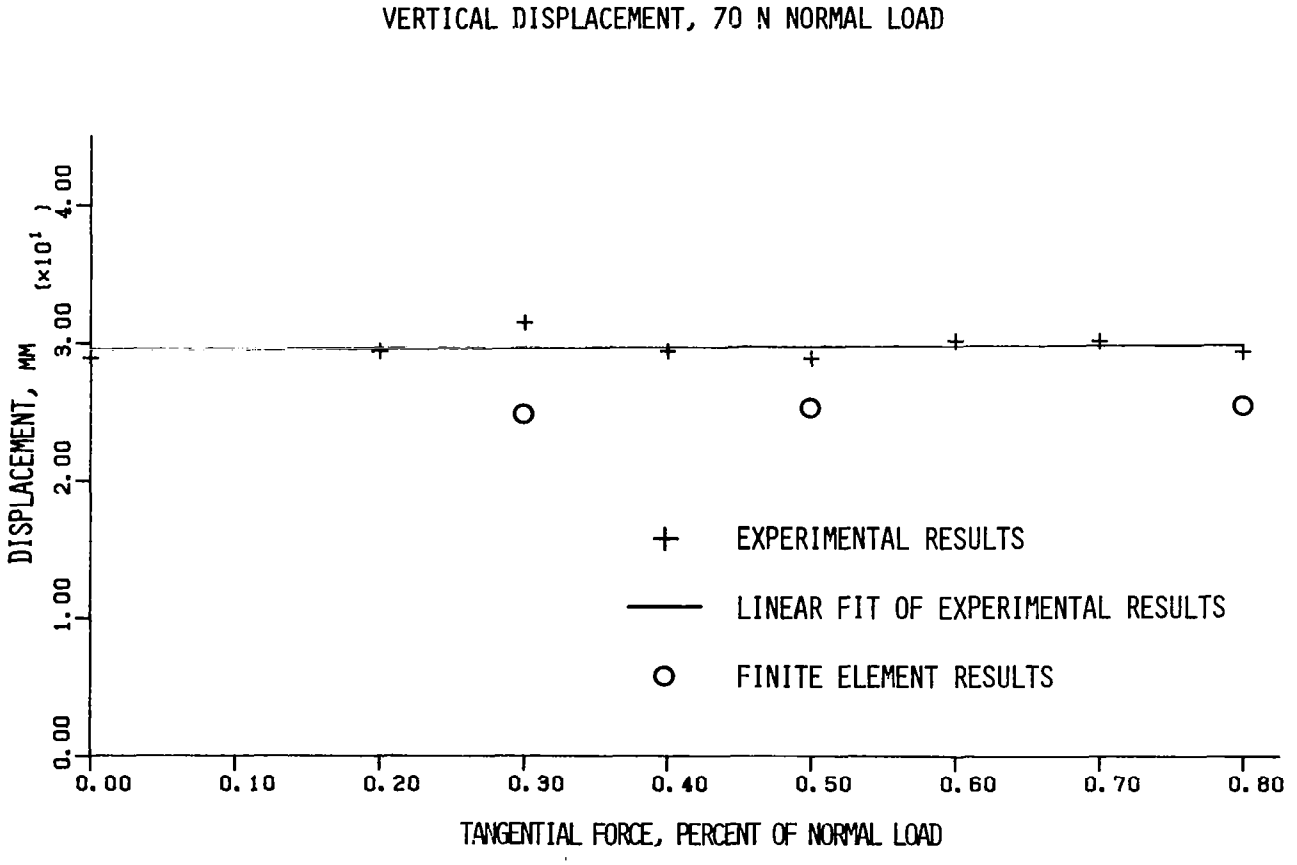

Figure 5

HORIZONTAL DISPLACEMENT OF TORUS

The graph of Figure 6 is similar to that of Figure 5 except that horizontal displacements of the torus are recorded rather than vertical displacements. A least squares cubic fit curve was chosen to best represent the experimental data after first considering both linear and quadratic forms. Of the three cases analyzed by finite element techniques, the first two are seen to agree remarkably well with the experimental results. For the greatest tangential force, however, STAGS predicts a horizontal displacement which is approximately only 50% of the measured value. Such a large discrepancy suggests that some undetected slip may have occurred between the lucite plate and inner tube for this case involving a high tangential braking force. Separate consideration of the three results arrived at by finite element analysis indicates the possibility of a more nearly linear relationship between horizontal displacement and tangential force. However, more data would have to be gathered before such a conclusion could be drawn.

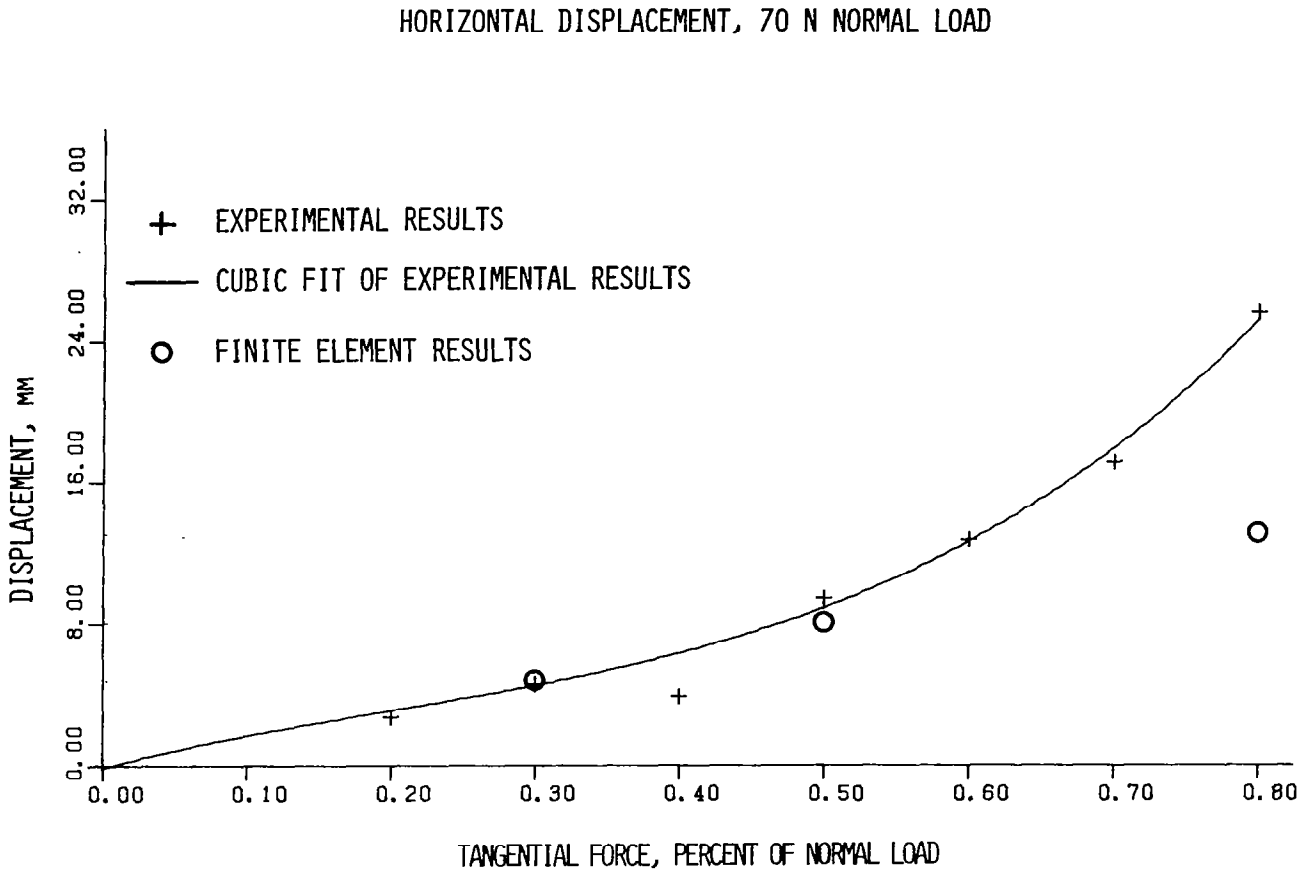

Figure 6

FINITE ELEMENT COORDINATES

Nominal dimensions of the inner tube used in this study are shown in Figure 7 along with the two coordinate angles required by STAGS to describe a toroidal shaped element. The angle θ is the circumferential angle. It varies from -180° to +180° for the torus. The meridional angle, α, varies from -42° to 90°. At α = -42° the torus is assumed to be clamped at the rim. Because there exists a plane of symmetry through the equator of the torus with respect to geometry as well as to the externally applied loads, it is possible to perform a complete finite element analysis by considering just half the inner tube. Hence, the maximum value for α is just 90° rather than 222°.

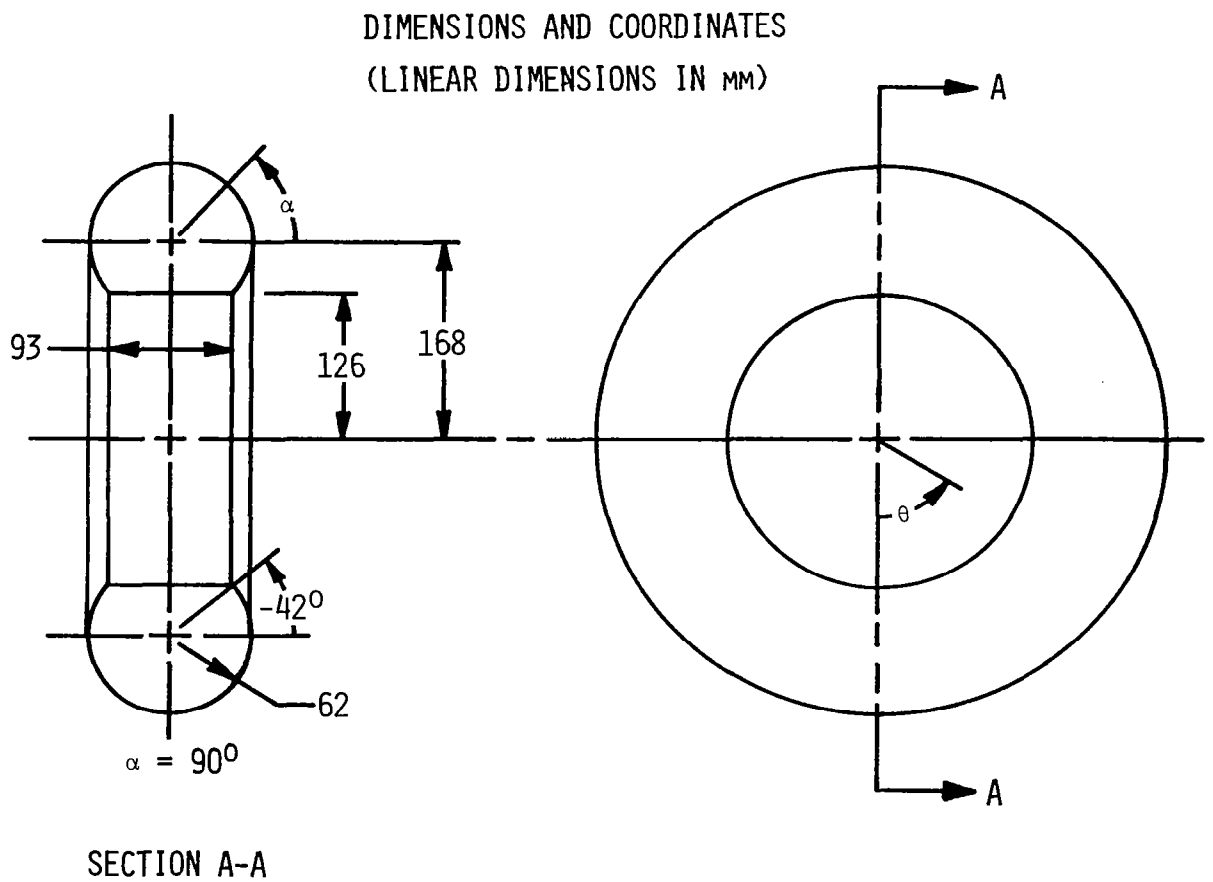

Figure 7

FINITE ELEMENT DISPLACEMENT RESULTS
FOR QUARTER TORUS WITH NORMAL LOAD

Shown in Figure 8 is the deformed as well as the undeformed geometry of the quarter torus analyzed by Mack (ref. 1) in a previous study. The finite element analysis was conducted with STAGS using a 13 x 15 grid pattern to define the location of the element nodes. A quarter torus was adequate in this case because there are two planes of symmetry in the absence of tangential loading. The 70 N normal load was evenly distributed over the nodes located within the experimentally determined footprint area. As can be seen, the evenly loaded nodes situated along the bottom of the torus in both views appear to lie on a relatively flat horizontal plane. Since the load plate is assumed to be horizontal and rigid, this result justified the use of an even load distribution in the footprint area for this particular case.

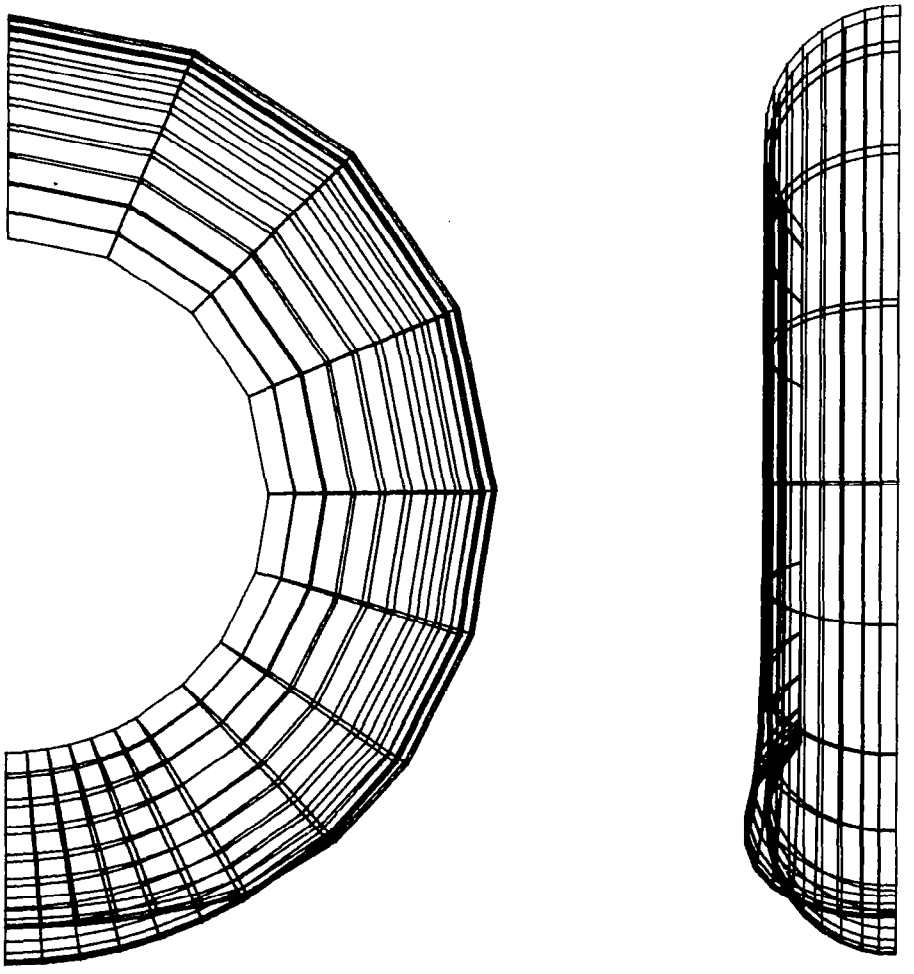

Figure 8

INITIAL RESULTS FROM FINITE ELEMENT DISPLACEMENT ANALYSIS WITH TANGENTIAL LOADING

The deformation of the half torus used to analyze the effect of combined normal and braking forces is illustrated in Figure 9. A 10 x 21 grid pattern was chosen in an attempt to provide a fine enough mesh for reasonably accurate results at a reasonable cost. The 70 N normal load is identical to that used for the quarter torus of Figure 8. In this initial run both the normal and tangential forces were evenly distributed over the nodes experimentally determined to lie within the footprint area. Unlike the normal load case of Figure 8, however, the loaded nodes along the bottom of the torus do not appear to lie on a horizontal plane. The tangential force, which acts to the left in the left-hand view, has the effect of tilting that portion of the toroidal surface meant to be in contact with the horizontal load plate. In an effort to correct this problem, an iterative method was devised to achieve a comparatively flat and horizontal surface across the bottom of the torus by systematically redistributing the forces on the nodes within the footprint area.

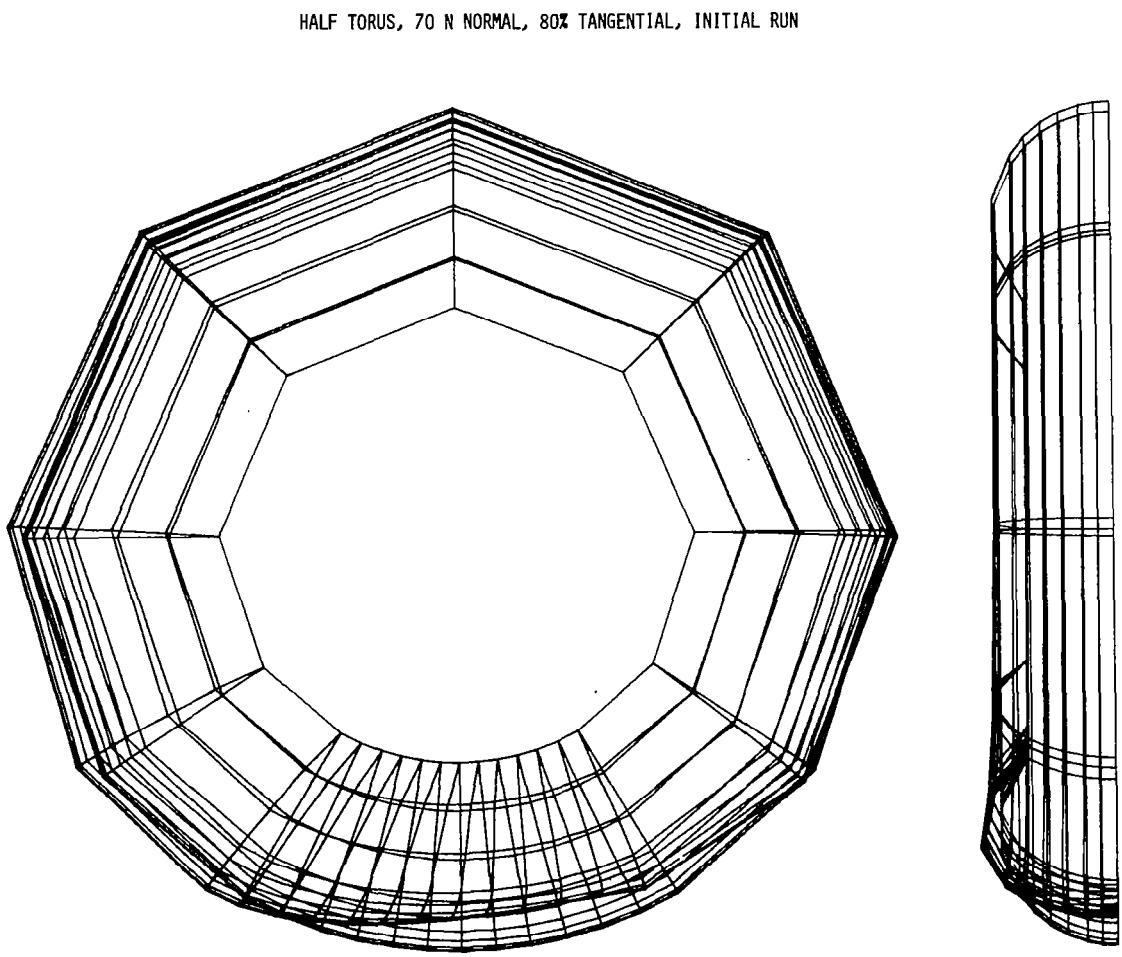

Figure 9

REDISTRIBUTION OF FORCES

The simplified model of Figure 10 illustrates the method developed to redistribute the forces in the footprint region. Suppose several springs of different lengths with different spring rates are suspended from a horizontal beam as shown. The total force to be exerted upward on the group of springs is known, and the individual forces to be applied to each of the springs is to be determined so that they all deflect to a common vertical equilibrium position denoted by Z_E. An arbitrary distribution of forces is chosen to begin the procedure. For example, the total force might initially be uniformly distributed over all the springs. The resulting deflection of each of the springs is observed, and a corresponding set of spring rates is calculated. From a consideration of the total force, the common equilibrium position, Z_E, is determined from the equation given in the lower right hand corner of the figure. Once Z_E is known the forces to be exerted on each of the individual springs are calculated from the equation provided for F_I. For a linear set of springs which act independently, these forces will, in fact, produce a common equilibrium position for all the springs. The situation with the inflated torus, however, is more complicated and requires an iterative scheme. The nodes within the footprint region are first loaded evenly. The STAGS analysis then gives the resulting deflections from which individual nodal spring rates are determined. A trial value is next computed for the equilibrium position just as in the case of the simplified model, and forces to be applied to the individual nodes are evaluated. These forces are then used to perform another STAGS analysis. Since the spring rates of the nodes are expected to be nonlinear, and since the nodes do not act independently, this second application of STAGS will not, in general, produce a flat, horizontal surface on the torus. Therefore, the entire procedure must be repeated until the deflected nodes are found to lie on a surface which is sufficiently flat and sufficiently horizontal.

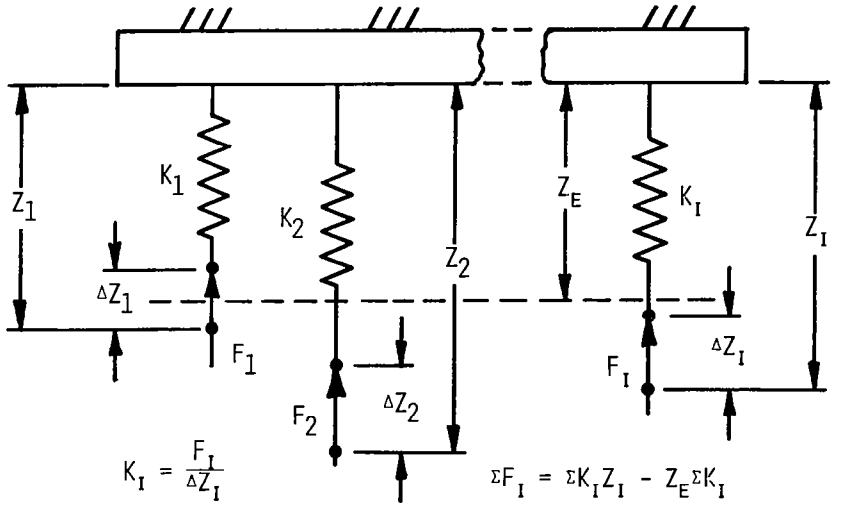

Figure 10

FINITE ELEMENT DISPLACEMENT ANALYSIS
FOR FIRST ITERATION

After redistributing the forces on the torus of Figure 9 by the method described in Figure 10, the STAGS analysis was performed again. The results of that analysis are shown in Figure 11. As can be seen, the footprint area is still not flat, but the severe tilt evident in Figure 9 has been greatly reduced.

HALF TORUS, 70 N NORMAL, 80% TANGENTIAL, FIRST ITERATION

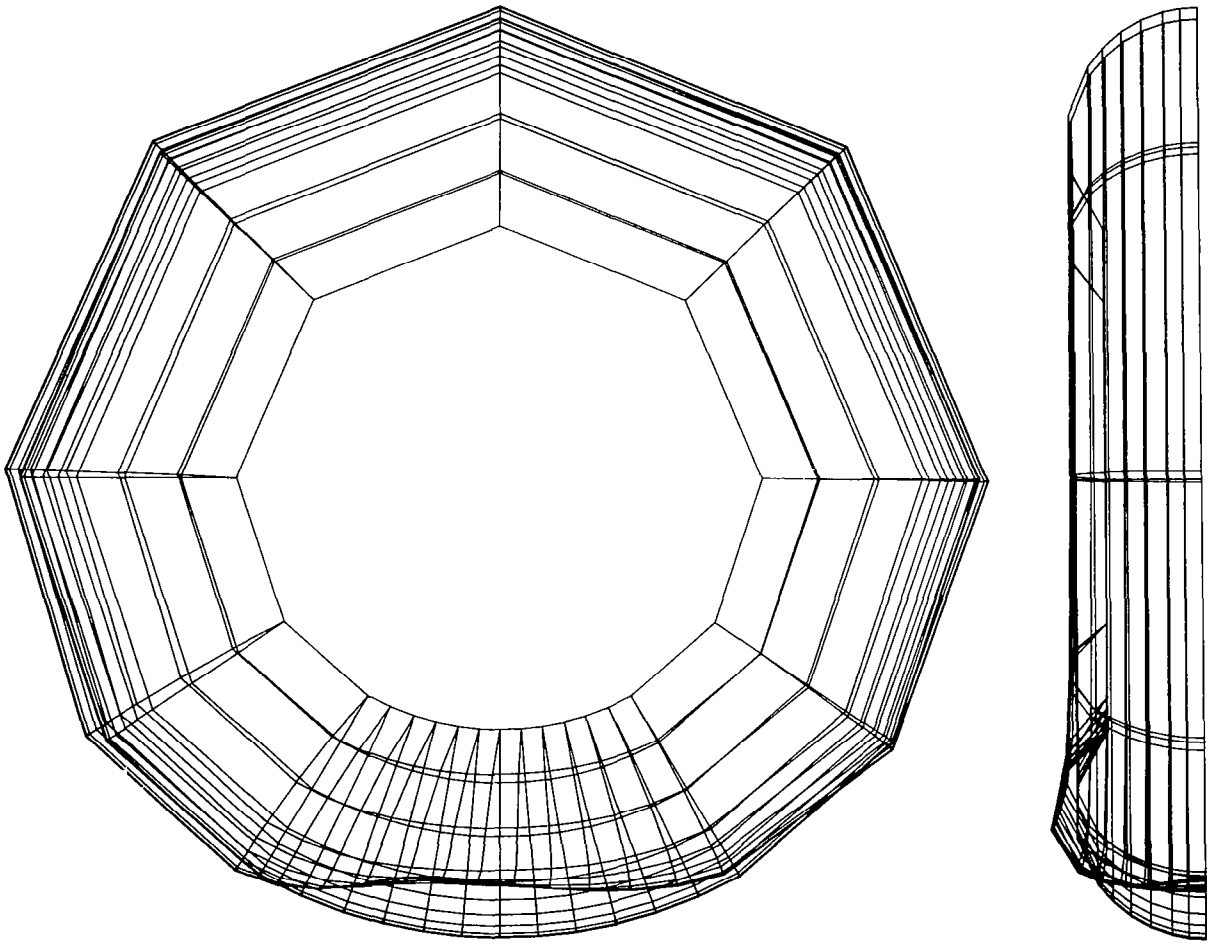

Figure 11

FINITE ELEMENT DISPLACEMENT ANALYSIS
FOR FINAL ITERATION

Figure 12 depicts the displacement results for the third iteration on the torus of Figures 9 and 11. Although some waviness is still apparent in the footprint region, the surface is relatively flat and horizontal. In fact, further iterations failed to produce any significant improvement. The common equilibrium position calculated for this case was used to establish the vertical deflection plotted in Figure 5 for a non-dimensional tangential force of 0.8. Only the normal components of force were considered in the redistribution process. Once the normal forces were established for each of the nodes, a tangential component of force equal to 0.8 of the corresponding normal force was added. Consequently, the resulting horizontal displacements of the nodes in the footprint region showed some variation. In order to arrive at a single value to characterize the horizontal deflection of the torus, the average of the horizontal displacements of the nodes across the center of the footprint area at a circumferential angle of 0° was computed. This value was then plotted in Figure 6 as one of the three data points found by the finite element method.

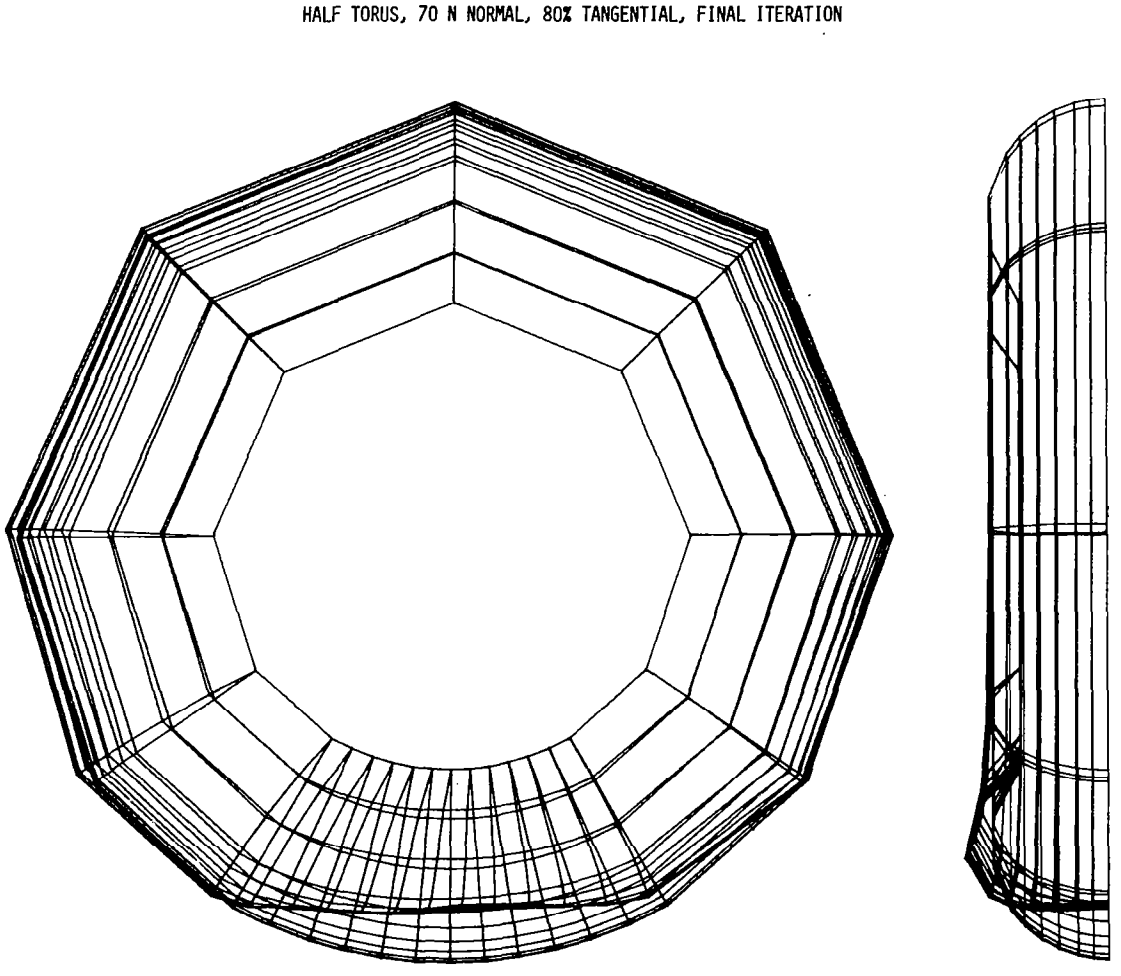

Figure 12

FORCE DISTRIBUTION FOR FINAL ITERATION

The footprint force distribution determined for the final iteration of Figure 12 is displayed in Figure 13. The sense of the tangential force applied to the torus is down and to the left with respect to the three dimensional plot. As shown, the force is greater along the sides of the footprint and at the left hand leading edge than in the middle. While the distribution appears to vary significantly, the minimum force at the middle of the footprint is actually 83% of the maximum force at the leading edge.

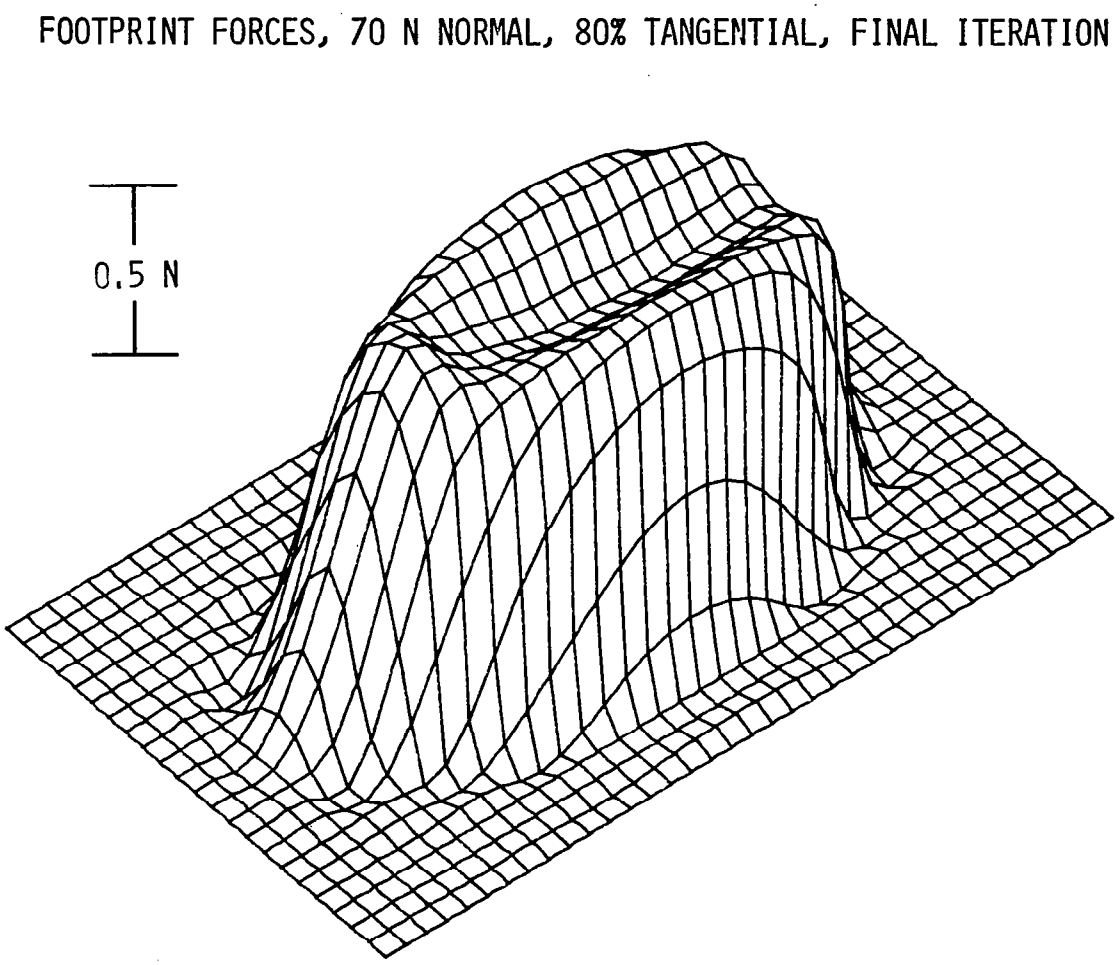

Figure 13

MERIDIONAL STRESSES FOR INITIAL RUN

The meridional stresses computed by STAGS for the initial run of Figure 9 are shown in Figure 14. The footprint area extends from approximately -25° to +25° in the circumferential direction and from approximately 90° to 45° in the meridional direction. The three dimensional display suggests the existence of a great deal of variation in the stresses throughout the torus with the stress even becoming compressive for a small area in the neighborhood of $\theta = 0°$. However, caution must be exercised in using this plot and those of the next three figures. There have been no experimental stress measurements made to verify these results, and no other grid patterns have as yet been tried to determine the effect of changing the finite element mesh on the computation of stresses. Another point that should be made with respect to Figures 14 through 17 is the fact that in executing the STAGS analysis the nodes located at circumferential angles of -180° and +180° were constrained to remain in a vertical plane. Hence, the stresses calculated at these extreme values of θ turned out to be quite different even though they represent the same points on the torus. Elimination of this constraint could have a significant effect on the predicted stress distribution.

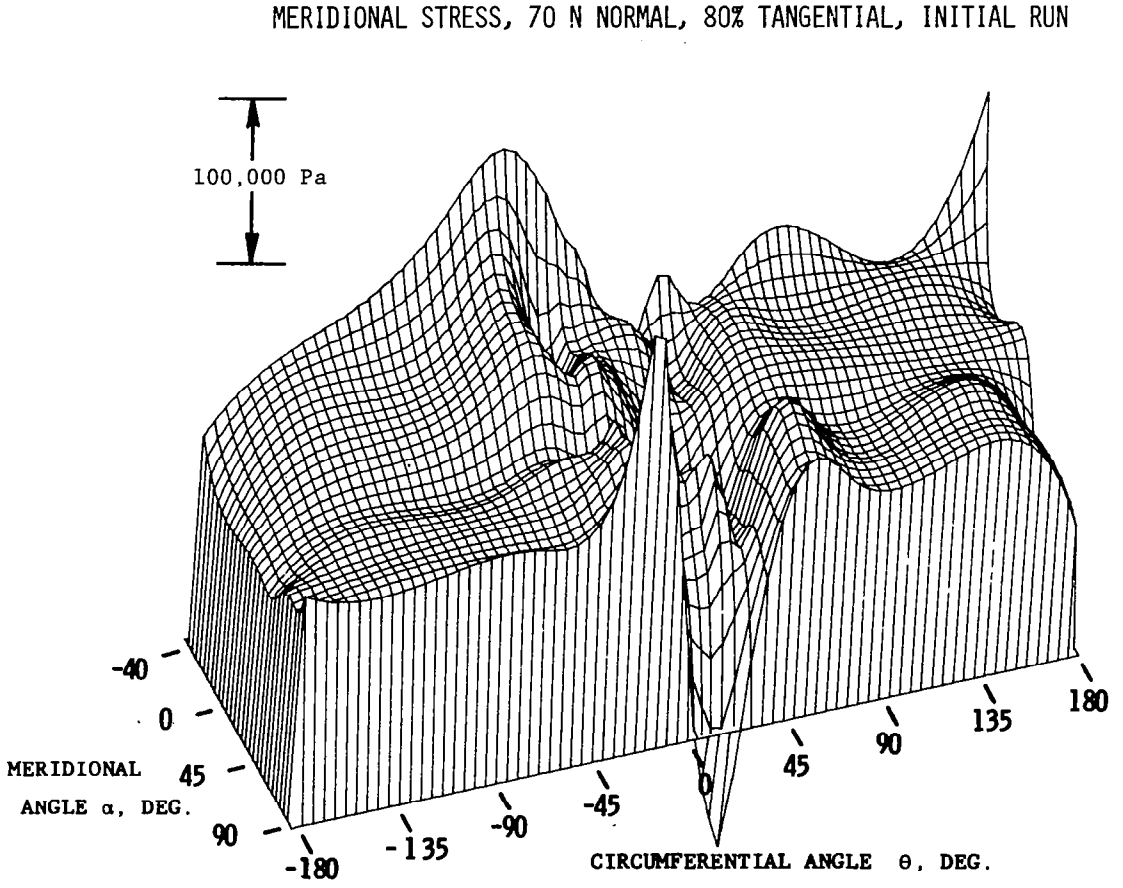

Figure 14

MERIDIONAL STRESSES FOR FINAL ITERATION

The meridional stresses for the final iteration of Figure 12 are depicted in Figure 15. Comparison with Figure 14 indicates that redistribution of the forces in the footprint area produces a dramatic effect on the stress distribution.

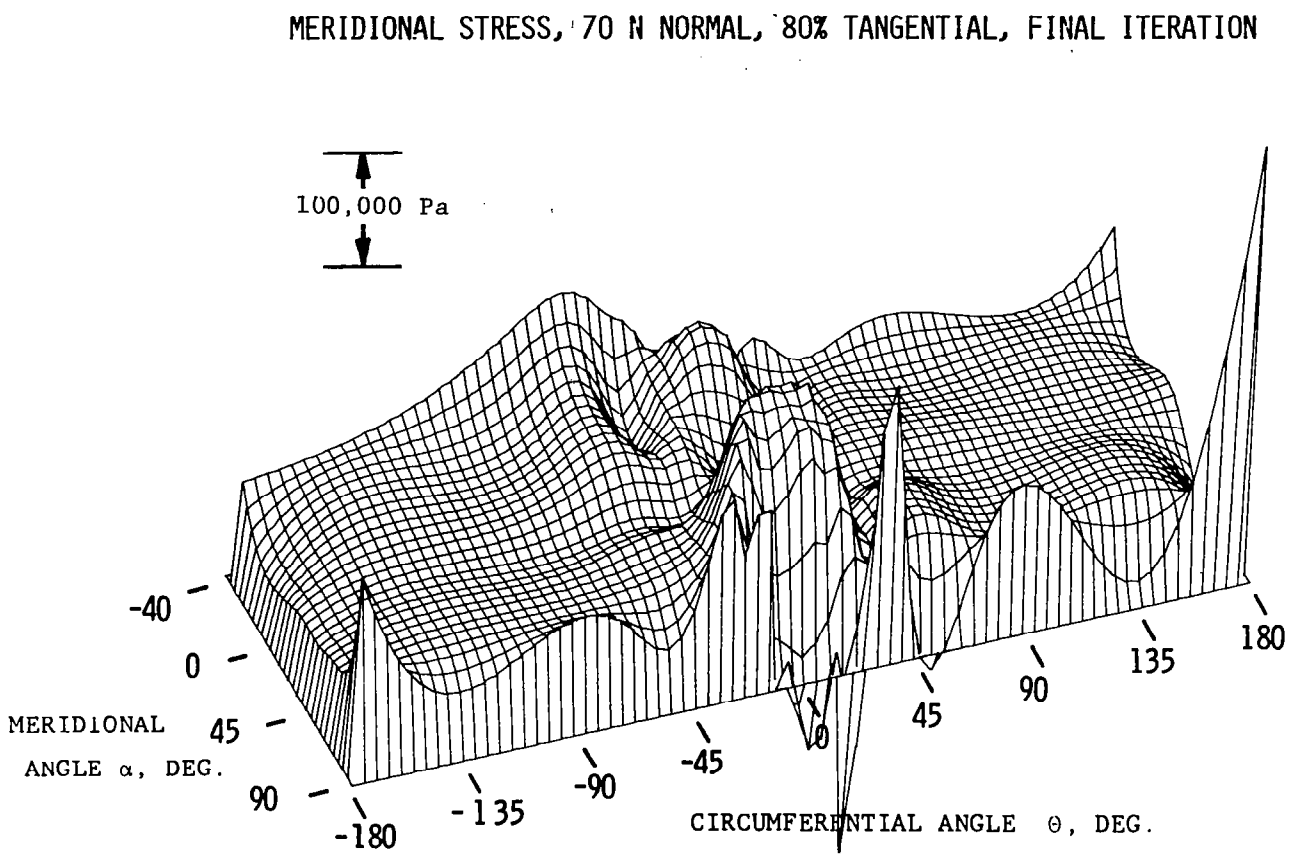

Figure 15

CIRCUMFERENTIAL STRESSES FOR INITIAL RUN

Figure 16 shows the circumferential stresses obtained from the STAGS analysis for the initial run of Figure 9. It is interesting to note the sharp decrease in stress at the leading edge of the footprint at a circumferential angle of approximately -40°. This seems reasonable in light of the fact that the tangential force is directed to the left with respect to the three dimensional plot.

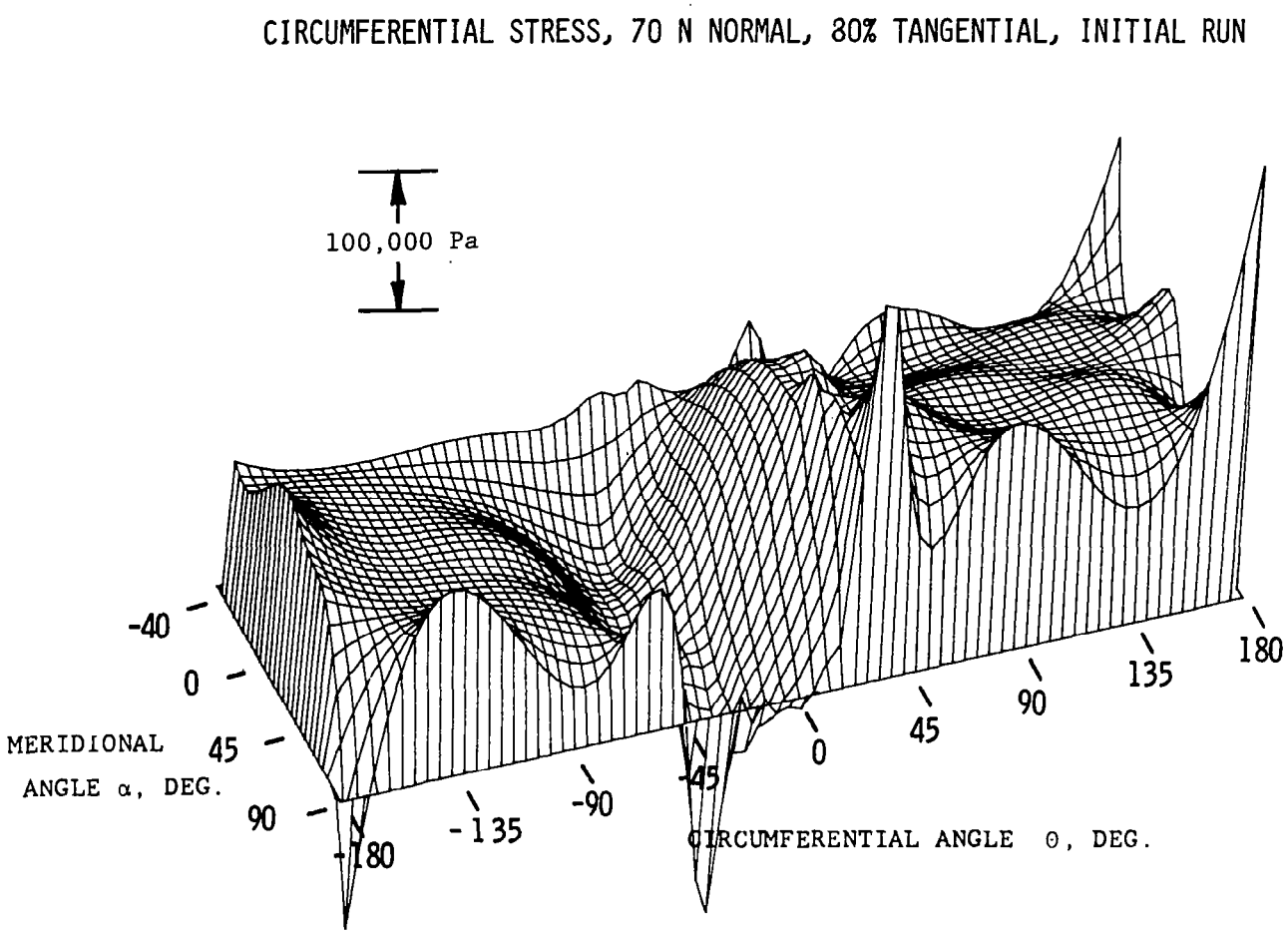

Figure 16

CIRCUMFERENTIAL STRESSES FOR FINAL ITERATION

Figure 17 depicts the circumferential stress results for the final iteration of Figure 12. The high stresses in the footprint region and the sharp decrease just to the left of the contact area are even more pronounced for this case with redistributed forces than for the initial run of Figure 16.

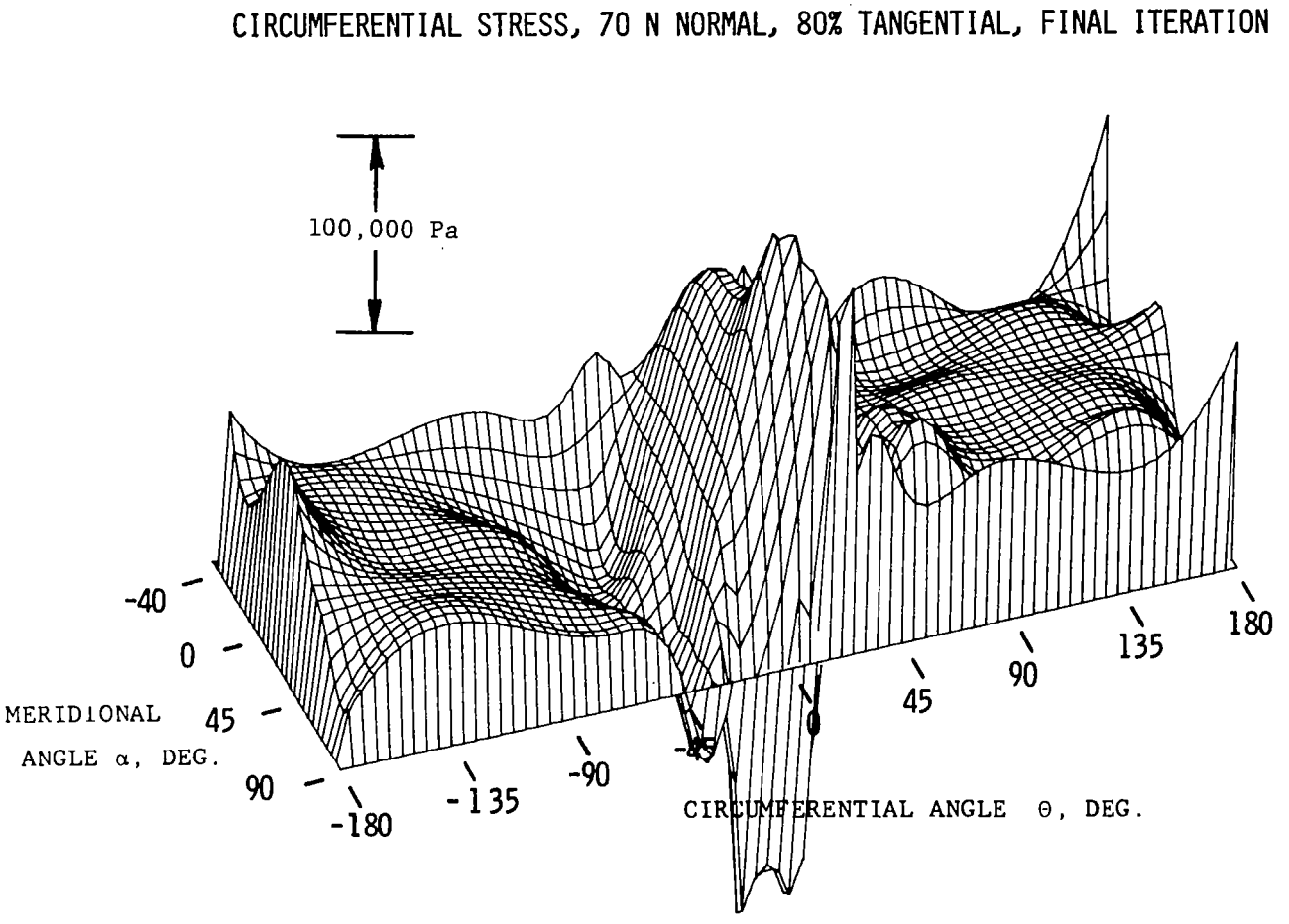

Figure 17

FINITE ELEMENT DISPLACEMENT RESULTS FOR INITIAL RUN OF SIX NODE CASE

In all the finite element work described thus far, the area of the footprint region was known beforehand from photographs taken on the test fixture of Figure 2. Nodes that were found to fall within the footprint area were then subjected to normal and tangential forces. In an attempt to eliminate the need to experimentally determine the contact area, a procedure was developed to start the iteration process described in Figure 10 by initially loading just six nodes centered about $\theta = 0°$ and $\alpha = 90°$. Theoretically, it should be possible to start with a single node, but it was decided that such a choice would only delay convergence to a final solution. The displacement results obtained when the full normal load of 70 N and the 80% tangential braking force were uniformly distributed over just six nodes are displayed in Figure 18. After spring rates were calculated for the six nodes and the first estimate of the common equilibrium position was determined, it was discovered that 102 nodes lay below Z_E. In the next run the total normal and tangential forces were evenly distributed over all 102 nodes. The next estimate of Z_E turned out to be considerably lower with only 83 nodes located below it. A second iteration reduced to 60 the number of nodes to be loaded. This corresponds to the number of nodes found experimentally to be within the footprint area for this particular load case. Three additional iterations were conducted to redistribute the forces by the method of Figure 10 in order to refine the flatness of the contact area.

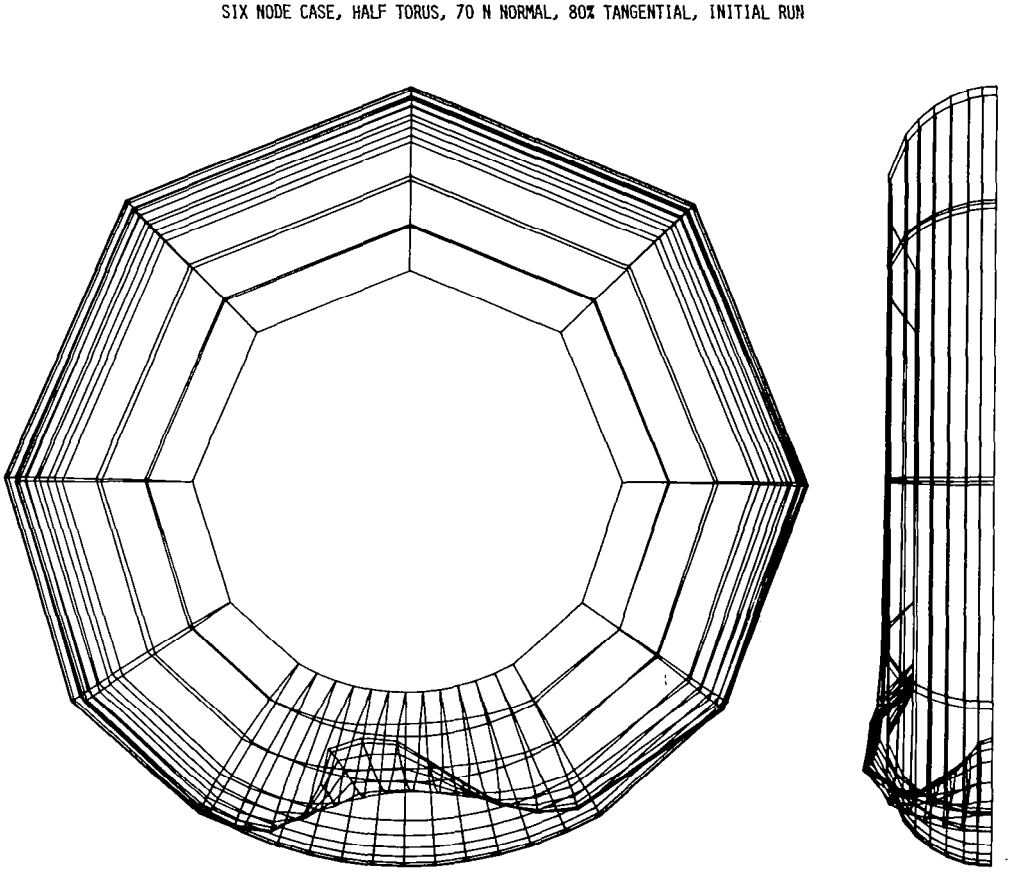

Figure 18

FINITE ELEMENT DISPLACEMENT RESULTS
FOR FINAL RUN OF SIX NODE CASE

The deformed geometry for the fifth iteration of the six node case is shown in Figure 19. Although not perfectly flat, the results are comparable to those of the final iteration depicted in Figure 12. While not included in this report, the final force distribution was also found to be very similar to that shown in Figure 13.

SIX NODE CASE, HALF TORUS, 70 N NORMAL, 80% TANGENTIAL, FINAL RUN

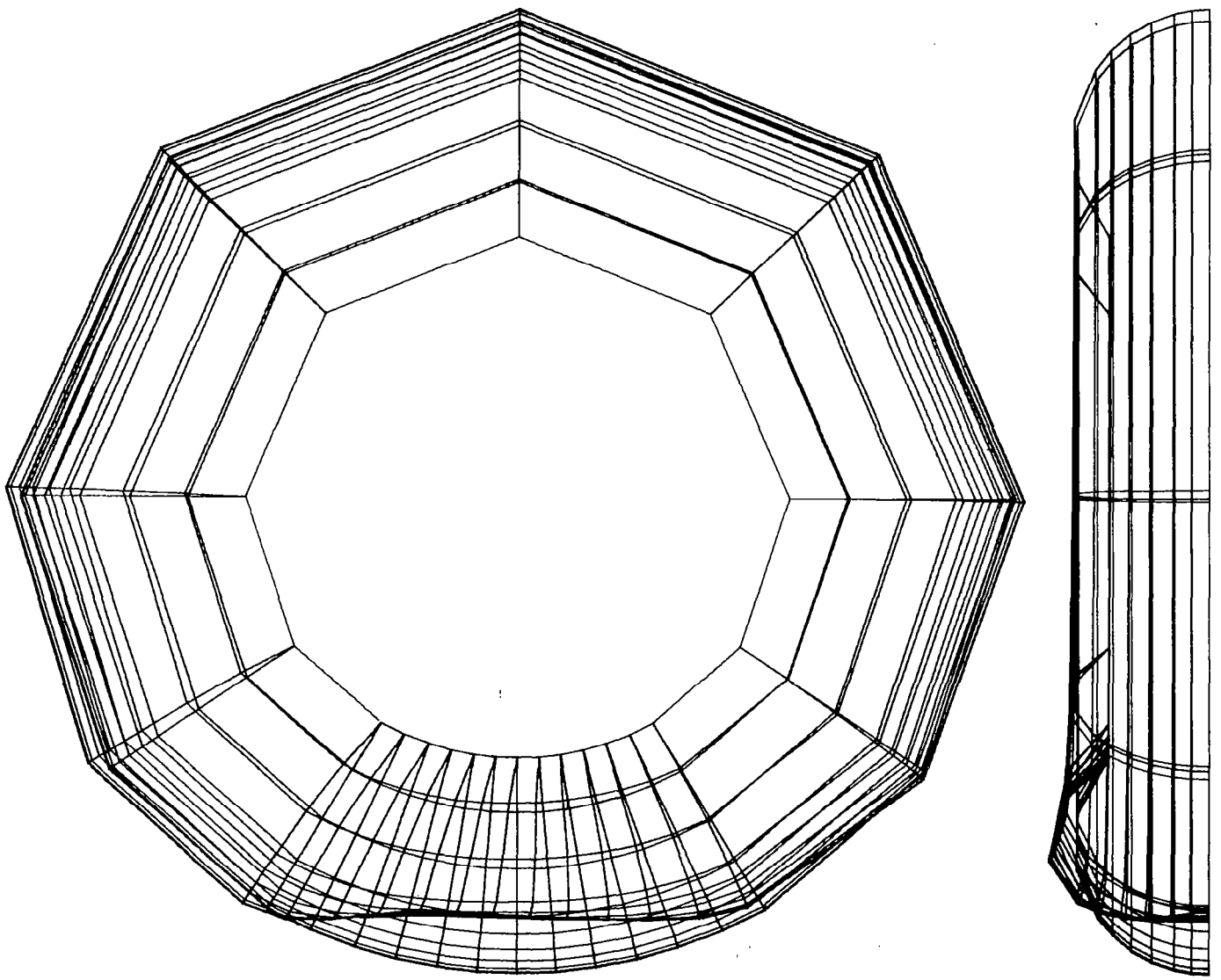

Figure 19

REFERENCES

1. Mack, M. J., Jr., "The Finite Element Analysis of an Inflated Toroidal Structure", M.S. Thesis, Dept. of Mechanical Engineering, Iowa State University, 1981.